

Quantum steering for two-mode states with continuous-variable in laser channel

Kaimin Zheng(郑凯敏), Jifeng Sun(孙继峰), Liyun Hu(胡利云), and Lijian Zhang(张利剑)
Citation: Chin. Phys. B, 2026, 35 (**2**): 020304. DOI: 10.1088/1674-1056/ae1820
http://cpb.iphy.ac.cn; http://iopscience.iop.org/cpb

What follows is a list of articles you may be interested in

Quantum manipulation of asymmetric Einstein-Podolsky-Rosen steering in controllable dynamical Casimir arrays

Ruinian Li(李瑞年), Yumei Long(龙玉梅), and Xue Zhang(张雪)
Chin. Phys. B, 2025, 34 (**2**): 020307. DOI: 10.1088/1674-1056/ad9a99

Generalized Einstein-Podolsky-Rosen steering paradox

Zhi-Jie Liu(刘志洁), Xing-Yan Fan(樊星言), Jie Zhou(周洁), Mi Xie(谢汨), and Jing-Ling Chen(陈景灵)
Chin. Phys. B, 2024, 33 (**11**): 110307. DOI: 10.1088/1674-1056/ad73b7

Ascertaining the influences of auxiliary qubits on the Einstein-Podolsky-Rosen steering and its directions

Ling-Ling Xing(邢玲玲), Huan Yang(杨欢), Gang Zhang(张刚), and Min Kong(孔敏)
Chin. Phys. B, 2024, 33 (**5**): 050304. DOI: 10.1088/1674-1056/ad1927

Genuine Einstein-Podolsky-Rosen steering of generalized three-qubit states via unsharp measurements

Yuyu Chen(陈玉玉), Fenzhuo Guo(郭奋卓), Shihui Wei(魏士慧), and Qiaoyan Wen(温巧燕)
Chin. Phys. B, 2023, 32 (**4**): 040309. DOI: 10.1088/1674-1056/acac14

Generation of tripartite Einstein-Podolsky-Rosen steering by cascaded nonlinear process

Yu Liu(刘瑜), Su-Ling Liang(梁素玲), Guang-Ri Jin(金光日), You-Bin Yu(俞友宾), Jian-Yu Lan(蓝建宇), Xiao-Bin He(何小斌), Kang-Xian Guo(郭康贤)
Chin. Phys. B, 2020, 29 (**5**): 050301. DOI: 10.1088/1674-1056/ab7da6

Quantum steering for two-mode states with continuous-variable in laser channel

Kaimin Zheng(郑凯敏)[1], Jifeng Sun(孙继峰)[2], Liyun Hu(胡利云)[2,†], and Lijian Zhang(张利剑)[1,‡]

[1] *National Laboratory of Solid State Microstructures, Key Laboratory of Intelligent Optical Sensing and Manipulation, College of Engineering and Applied Sciences, and Collaborative Innovation Center of Advanced Microstructures, Nanjing University, Nanjing* 210023, *China*
[2] *Center for Quantum Science and Technology, Jiangxi Normal University, Nanchang* 330022, *China*

(Received 17 September 2025; revised manuscript received 27 October 2025; accepted manuscript online 28 October 2025)

Einstein–Podolsky–Rosen (EPR) steering is an important resource for one-sided device-independent quantum information processing. This steering property can be destroyed by the interaction between a quantum system and its environment in practical applications. In this paper, we employ the characteristic function representation of probability distributions to investigate the quantum steering of two-mode continuous-variable states in a laser channel, where both the gain factor and the loss effect are taken into account. Firstly, we analyse the steering time of the two-mode squeezed vacuum state under one-mode and two-mode laser channels, respectively. We find that the gain process introduces additional noise into the two-mode squeezed vacuum state, thereby reducing the steerable time. Secondly, by quantifying EPR steering, we show that two-side loss exhibits smaller steerability than one-side loss, although they share the same two-way steerable time. In addition, we find that the more-gained party can steer the other party's state, whereas the other party cannot steer the gained party beyond a certain threshold value. In this sense, the gain effect in one party appears to be equivalent to the loss effect in the other party. Our results pave the way for the distillation of EPR steering and quantum information processing in practical quantum channels.

Keywords: Einstein–Podolsky–Rosen steering, laser channel, characteristic function

PACS: 03.65.Ud, 03.65.Yz, 03.67.–a, 03.67.Hk

DOI: 10.1088/1674-1056/ae1820 **CSTR:** 32038.14.CPB.ae1820

1. Introduction

The Einstein–Podolsky–Rosen (EPR) steering was first proposed by Schrödinger in 1935 in response to the famous paper by Einstein, Podolsky, and Rosen on the completeness of quantum mechanics.[1] It allows the subsystem Alice to steer the quantum state of a distant subsystem Bob through local measurements.[2–6] In terms of the degree of quantum correlation, EPR steering is intermediate between Bell inequality and quantum entanglement.[7,8] Unlike Bell inequality and quantum entanglement, EPR steering is inherently asymmetric for two subsystems, i.e., the ability of Alice to steer Bob may be different from the ability of Bob to steer Alice, and there may even be a one-way EPR steering situation.[9–14] EPR steering has received increasing attention since Wiseman *et al.*[7] analyzed quantum entanglement, EPR steering and Bell inequality separately from the perspective of quantum information tasks.

One important element of research on quantum EPR steering is to demonstrate the existence of one-way steering. In terms of discrete-variable systems, one-way EPR steering was first demonstrated with Werner states and has been proved by using the "all-or-nothing proof" criterion and quantum storage.[15,16] Pan *et al.*[17] have demonstrated true four-body EPR steering and its application to one-way quantum computing. For continuous-variable systems, the existence of one-way EPR steering based on Reid's criterion was first demonstrated by introducing one-sided loss in a two-mode squeezed state.[18] On this basis, Su *et al.*[19,20] have successfully realized free control of EPR steering by using noise, and many-body Gaussian EPR steering has been observed by introducing asymmetric losses. On the other hand, the interaction between a quantum system and its environment is inevitable for quantum information processing in practical quantum channels. Thus, it is crucial to investigate the effect of decoherence on EPR steering in quantum channels, which can help to design effective distillation programmes. The decoherence of EPR steering has been theoretically analysed and experimentally demonstrated in recent years.[21–26] Most existing studies only take into account lossy and noisy channels. However, quantum tasks in free space encounter challenges beyond simple loss channels. For instance, satellite-based quantum teleportation is subject to atmospheric turbulence, which is typically modeled by a laser channel or a phase-sensitive channel.[27,28] Hence, to enable reliable quantum information processing (QIP) over such channels, it is essential to analyze the evolution of EPR steering and entanglement resources under these specific conditions. This investigation provides a the-

†Corresponding author. E-mail: hlyun@jxnu.edu.cn
‡Corresponding author. E-mail: lijian.zhang@nju.edu.cn

© 2026 Chinese Physical Society and IOP Publishing Ltd. All rights, including for text and data mining, AI training, and similar technologies, are reserved.

oretical foundation for designing more effective QIP protocols with enhanced fidelity and robustness.

We first derive the relation between probability distribution functions and the characteristic function in Section 2. This relation provides a relatively easy approach for obtaining analytical expressions of the EPR steering criterion for the two-mode squeezed vacuum state. In Section 3, we analyse the steering conditions of the two-mode squeezed vacuum state under a laser channel. In Section 4, we further analyse the relationship between the magnitude of EPR steering and the parameters of the laser channel. In Section 5, we compare the decoherence of quantum steering and entanglement in a laser channel. In Section 6, we extend our discussion to the evolution of the TMSV in the presence of a phase-sensitive environment. Lastly, in Section 7, we give concluding remarks.

2. The EPR steering criterion

2.1. Relation between PDFs and CF

In quantum steering criteria, the probability distribution functions (PDFs) are usually employed in the calculation of the original Reid criterion, entropic steering criterion, and Adesso's steering lower bound for Gaussian states. In addition, it is worth noting that the characteristic function (CF) provides a relatively easy way to obtain analytical expressions for expectation values, especially for systems in noisy environments. Here, we therefore first derive the relation between PDFs and CF.

For a two-mode quantum system ρ, its Weyl expression of the density operator is given by

$$\begin{aligned}\rho \;=\; & \int_{-\infty}^{\infty}\frac{\mathrm{d}q_1\,\mathrm{d}p_1\,\mathrm{d}q_2\,\mathrm{d}p_2}{\pi^2}\chi\left(q_1,p_1;q_2,p_2\right)\\ & \times D_1\left(-q_1,-p_1\right)D_2\left(-q_2,-p_2\right),\end{aligned}\tag{1}$$

where $\chi\left(q_1,p_1;q_2,p_2\right)=\mathrm{tr}\left[\rho D_1\left(q_1,p_1\right)D_2\left(q_2,p_2\right)\right]$ is the CF, and $D_l\left(q_l,p_l\right)$ $(l=1,2)$ are the displacement operators. In addition, $D_l\left(q_l,p_l\right)$ can be expressed as

$$\begin{aligned}D_l\left(q_l,p_l\right) \;&=\; \mathrm{e}^{\mathrm{i}\left(p_lQ_l-q_lP_l\right)}\\ &=\; \mathrm{e}^{-\mathrm{i}q_lp_l}\,\mathrm{e}^{\mathrm{i}p_lQ_l}\,\mathrm{e}^{-\mathrm{i}q_lP_l}\\ &=\; \mathrm{e}^{\mathrm{i}q_lp_l}\,\mathrm{e}^{-\mathrm{i}q_lP_l}\,\mathrm{e}^{\mathrm{i}p_lQ_l},\end{aligned}\tag{2}$$

where $Q_l=a_l+a_l^{\dagger}$ and $P_l=\left(a_l-a_l^{\dagger}\right)/\mathrm{i}$ are the coordinate and momentum operators, respectively, satisfying $[Q_l,P_l]=2\mathrm{i}$. From Eq. (2) and noting that $\mathrm{e}^{-\mathrm{i}q_lP_l}\left|\bar{q}_l\right\rangle=\left|\bar{q}_l+\sqrt{2}q_l\right\rangle$, as well as $\mathrm{e}^{\mathrm{i}p_lQ_l}\left|\bar{p}_l\right\rangle=\left|\bar{p}_l+\sqrt{2}p_l\right\rangle$, it is straightforward to obtain

$$\left\langle\bar{q}_l\right|D_l\left(q_l,p_l\right)\left|\bar{q}_l\right\rangle=\mathrm{e}^{\mathrm{i}\sqrt{2}\bar{q}_lp_l}\,\delta\left(\sqrt{2}q_l\right),\tag{3}$$

$$\left\langle\bar{p}_l\right|D_l\left(q_l,p_l\right)\left|\bar{p}_l\right\rangle=\mathrm{e}^{-\mathrm{i}\sqrt{2}q_l\bar{p}_l}\,\delta\left(\sqrt{2}p_l\right),\tag{4}$$

where $\left|\bar{q}_l\right\rangle$ and $\left|\bar{p}_l\right\rangle$ are the eigenstates of Q_l and P_l, respectively, i.e., $Q_l\left|\bar{q}_l\right\rangle=\sqrt{2}\bar{q}_l\left|\bar{q}_l\right\rangle$ and $P_l\left|\bar{p}_l\right\rangle=\sqrt{2}\bar{p}_l\left|\bar{p}_l\right\rangle$.

After substituting Eqs. (3) and (4) into Eq. (1), the joint PDFs, as well as their marginal and conditional PDFs, can be readily calculated. For instance,

$$\begin{aligned}P\left(\bar{q}_1,\bar{q}_2\right) \;&=\; \left\langle\bar{q}_1,\bar{q}_2\right|\rho\left|\bar{q}_1,\bar{q}_2\right\rangle\\ &=\; \int_{-\infty}^{\infty}\frac{\mathrm{d}p_1\,\mathrm{d}p_2}{2\pi^2}\,\mathrm{e}^{-\mathrm{i}\sqrt{2}\left(\bar{q}_1p_1+\bar{q}_2p_2\right)}\chi\left(0,p_1;0,p_2\right),\\ P\left(\bar{p}_1,\bar{p}_2\right) \;&=\; \left\langle\bar{p}_1,\bar{p}_2\right|\rho\left|\bar{p}_1,\bar{p}_2\right\rangle\\ &=\; \int_{-\infty}^{\infty}\frac{\mathrm{d}q_1\,\mathrm{d}q_2}{2\pi^2}\,\mathrm{e}^{\mathrm{i}\sqrt{2}\left(\bar{p}_1q_1+\bar{p}_2q_2\right)}\chi\left(q_1,0;q_2,0\right),\end{aligned}\tag{5}$$

and

$$\begin{aligned}P\left(\bar{q}_1\right) \;&=\; \int_{-\infty}^{\infty}\mathrm{d}\bar{q}_2P\left(\bar{q}_1,\bar{q}_2\right)\\ &=\; \frac{1}{\sqrt{2}\pi}\int_{-\infty}^{\infty}\mathrm{d}p_1\,\mathrm{e}^{-\mathrm{i}\sqrt{2}\bar{q}_1p_1}\chi\left(0,p_1;0,0\right),\\ P\left(\bar{p}_1\right) \;&=\; \int_{-\infty}^{\infty}\mathrm{d}\bar{p}_2P\left(\bar{p}_1,\bar{p}_2\right)\\ &=\; \frac{1}{\sqrt{2}\pi}\int_{-\infty}^{\infty}\mathrm{d}q_1\,\mathrm{e}^{\mathrm{i}\sqrt{2}\bar{p}_1q_1}\chi\left(q_1,0;0,0\right),\end{aligned}\tag{6}$$

as well as

$$P\left(\bar{q}_2\middle|\bar{q}_1\right)=P\left(\bar{q}_1,\bar{q}_2\right)/P\left(\bar{q}_1\right).\tag{7}$$

Thus, the inferred variance of Q can be derived as

$$\begin{aligned}&\Delta_{\mathrm{inf}}^2\left(Q_2|Q_1\right)\\ \equiv\;& \int_{-\infty}^{\infty}\mathrm{d}\bar{q}_1P\left(\bar{q}_1\right)\Delta_{\mathrm{inf}}^2\left(Q_2|Q_1=\bar{q}_1\right)\\ =\;& \int_{-\infty}^{\infty}\mathrm{d}\bar{q}_1P\left(\bar{q}_1\right)\int_{-\infty}^{\infty}\mathrm{d}\bar{q}_2P\left(\bar{q}_2|\bar{q}_1\right)\left(\bar{q}_2-q_{\mathrm{est}}\right)^2\\ =\;& \int_{-\infty}^{\infty}\mathrm{d}\bar{q}_1\,\mathrm{d}\bar{q}_2P\left(\bar{q}_1,\bar{q}_2\right)\left(\bar{q}_2-q_{\mathrm{est}}\right)^2.\end{aligned}\tag{8}$$

Here q_{est} is a function of the variable $\bar{q}_1$.

2.2. Reid criterion

Using linear inference, i.e., taking $q_{\mathrm{est}}=d-\lambda\bar{q}_1$, where the two parameters λ and d are chosen to minimize the inferred variance $\Delta_{\mathrm{inf}}^2\left(Q_2|Q_1\right)$, a straightforward calculation yields

$$\begin{aligned}\Delta_{\mathrm{inf}}^2\left(Q_2|Q_1\right) \;=\; & \frac{1}{2}\lambda^2\left\langle Q_1^2\right\rangle+\lambda\left\langle Q_1Q_2\right\rangle-\sqrt{2}\lambda d\left\langle Q_1\right\rangle\\ & +d^2-\sqrt{2}d\left\langle Q_2\right\rangle+\frac{1}{2}\left\langle Q_2^2\right\rangle,\end{aligned}\tag{9}$$

where we have used the relation between the CF and the expectation values, for instance

$$\left\langle Q_2\right\rangle=\left.\frac{\partial}{\partial\left(\mathrm{i}p_2\right)}\chi\left(0,0;0,p_2\right)\right|_{p_2=0},\tag{10}$$

$$\left\langle Q_2^2\right\rangle=\left.\frac{\partial^2}{\partial\left(\mathrm{i}p_2\right)^2}\chi\left(0,0;0,p_2\right)\right|_{p_2=0},\tag{11}$$

$$\langle Q_1 Q_2\rangle = \frac{-\partial^2}{\partial p_1 \partial p_2}\chi(0,p_1;0,p_2)\Big|_{p_1,p_2=0}. \tag{12}$$

The parameters λ and d are determined by minimizing $\Delta^2_{\inf}(Q_2|Q_1)$, such that $\frac{\partial}{\partial\lambda}\Delta^2_{\inf}(Q_2|Q_1) = \frac{\partial}{\partial d}\Delta^2_{\inf}(Q_2|Q_1) = 0$, which yields

$$\lambda = -\frac{E_{Q_1Q_2}}{V(Q_1)},\ d = \frac{\lambda\langle Q_1\rangle + \langle Q_2\rangle}{\sqrt{2}}, \tag{13}$$

where $E_{Q_1Q_2} = \langle Q_1Q_2\rangle - \langle Q_1\rangle\langle Q_2\rangle$ and $V(Q_l) = \langle Q_l^2\rangle - \langle Q_l\rangle^2$ is the variance of Q_l ($l = 1,2$). Substituting Eq. (13) into Eq. (9), the minimized inferred variance $\Delta^2_{\min}(Q_2|Q_1)$ is obtained as

$$\Delta^2_{\min}(Q_2|Q_1) = \frac{1}{2}\left(V(Q_2) - \frac{(E_{Q_1Q_2})^2}{V(Q_1)}\right), \tag{14}$$

The minimized inferred variance $\Delta^2_{\min}(P_2|P_1)$ can be derived in a similar manner as

$$\Delta^2_{\min}(P_2|P_1) = \frac{1}{2}\left(V(P_2) - \frac{(E_{P_1P_2})^2}{V(P_1)}\right), \tag{15}$$

where $V(P_l) = \langle P_l^2\rangle - \langle P_l\rangle^2$ and $E_{P_1P_2} = \langle P_1P_2\rangle - \langle P_1\rangle\langle P_2\rangle$. Combining Eqs. (14) and (15) and employing the Heisenberg uncertainty relation yields the Reid inequality (RI)

$$V_{B|A} \equiv \Delta^2_{\min}(Q_2|Q_1)\Delta^2_{\min}(P_2|P_1) \geqslant \frac{1}{4}, \tag{16}$$

where the commutation relations $[Q_l,P_l] = 2\mathrm{i}$ are used. Thus, the EPR paradox — or steering — occurs when the RI is violated.

In a similar way, if Bob aims to infer Alice's measurement outcomes, the RI reads

$$V_{A|B} \equiv \Delta^2_{\min}(Q_1|Q_2)\Delta^2_{\min}(P_1|P_2) \geqslant \frac{1}{4}, \tag{17}$$

with

$$\Delta^2_{\min}(Q_1|Q_2) = \frac{1}{2}\left(V(Q_1) - \frac{(E_{Q_1Q_2})^2}{V(Q_2)}\right), \tag{18}$$

$$\Delta^2_{\min}(P_1|P_2) = \frac{1}{2}\left(V(P_1) - \frac{(E_{P_1P_2})^2}{V(P_2)}\right). \tag{19}$$

From Eqs. (14)–(19), it is evident that once the CF is known, $V_{B|A}$ and $V_{A|B}$ can be directly evaluated using Eqs. (10)–(12). In addition, for Gaussian states, which are fully characterized by their covariance matrices, the quantities involved in the inferred variances can be directly extracted from the covariance matrix.

2.3. RI violation of two-mode squeezed vacuum state

Next, we consider a two-mode squeezed vacuum (TMSV) state $|\mathrm{TMSV}\rangle$, which can be generated via a nondegenerate optical parametric process, i.e.

$$|\mathrm{TMSV}\rangle = S(r)|00\rangle, \tag{20}$$

where $S(r) = \exp(r(a_1^\dagger a_2^\dagger - a_1a_2))$ is the two-mode squeezing operator. The corresponding CF is given by

$$\chi_{\mathrm{TMSV}} = \exp\left(-\frac{1}{2}(q_1^2+q_2^2+p_1^2+p_2^2)\cosh 2r\right) \times \exp((q_1q_2 - p_1p_2)\sinh 2r). \tag{21}$$

Using Eqs. (10)–(12), one readily obtains

$$\Delta^2_{\min}(Q_2|Q_1) = \Delta^2_{\min}(P_2|P_1) = \frac{1}{2\cosh 2r}, \tag{22}$$

which leads to

$$V_{B|A} = \frac{1}{4\cosh^2 2r} < \frac{1}{4}. \tag{23}$$

Thus, the TMSV state exhibits EPR steering for any nonzero squeezing. Here we note that the Reid criterion depends only on second-order moments of observables, which implies that it is particularly effective for Gaussian states, since Gaussian states are fully characterized by their second-order moments or covariance matrices. However, this is not the case for non-Gaussian states, whose characterization also involves higher-order moments.

2.4. Entropic steering criterion

To more effectively demonstrate EPR steering, especially for non-Gaussian states, correlations of all orders should be involved in the steering criterion. Based on the entropic uncertainty relation[29]

$$H(Q) + H(P) \geqslant \ln(\mathrm{e}\pi), \tag{24}$$

where $H(Y)$ ($Y = Q,P$ representing observables) is the Shannon entropy of the $y\,(=q,p)$ PDF, i.e.

$$H(Y) = -\int \mathrm{d}y P(y)\ln P(y), \tag{25}$$

Walborn *et al.*[30] have derived an entropic steering inequality, i.e., for instance, for the position and momentum distributions

$$H_{B|A} \equiv H(Q_2|Q_1) + H(P_2|P_1) \geqslant \ln(\mathrm{e}\pi), \tag{26}$$

where the conditional entropies $H(Q_2|Q_1)$ and $H(P_2|P_1)$ are respectively given by

$$H(Q_2|Q_1) = H(Q_1,Q_2) - H(Q_1), \tag{27}$$

$$H(P_2|P_1) = H(P_1,P_2) - H(P_1), \tag{28}$$

with

$$H(x_1) = -\int \mathrm{d}x_1 P(x_1)\ln P(x_1), \tag{29}$$

$$H(x_1,x_2) = -\int \mathrm{d}x_1\,\mathrm{d}x_2 P(x_1,x_2)\ln P(x_1,x_2). \tag{30}$$

Next, we consider the inferred Shannon entropy $H_{B|A}$ for the TMSV state defined in Eq. (20) as an example. Using the CF of the TMSV in Eq. (21) and Eqs. (5) and (6), one readily obtains

$$P(\bar{q}_1) = \frac{1}{\sqrt{\pi \cosh 2r}} \mathrm{e}^{-\bar{q}_1^2 \operatorname{sech} 2r}, \tag{31}$$

$$P(\bar{p}_1) = \frac{1}{\sqrt{\pi \cosh 2r}} \mathrm{e}^{-\bar{p}_1^2 \operatorname{sech} 2r}, \tag{32}$$

and

$$P(\bar{q}_1, \bar{q}_2) = \frac{1}{\pi} \mathrm{e}^{-(\bar{q}_1^2+\bar{q}_2^2)\cosh 2r + 2\bar{q}_1\bar{q}_2 \sinh 2r}, \tag{33}$$

$$P(\bar{p}_1, \bar{p}_2) = \frac{1}{\pi} \mathrm{e}^{-(\bar{p}_1^2+\bar{p}_2^2)\cosh 2r - 2\bar{p}_1\bar{p}_2 \sinh 2r}, \tag{34}$$

which yield

$$H(Q_1) = H(P_1) = \ln \sqrt{\pi \mathrm{e} \cosh 2r}, \tag{35}$$

$$H(Q_1, Q_2) = H(P_1, P_2) = \ln(\mathrm{e}\pi), \tag{36}$$

and

$$H(Q_2|Q_1) = H(P_2|P_1) = \frac{1}{2} \ln \frac{\mathrm{e}\pi}{\cosh 2r}, \tag{37}$$

as well as

$$H(Q_2|Q_1) + H(P_2|P_1) = \ln \frac{\mathrm{e}\pi}{\cosh 2r} < \ln(\mathrm{e}\pi), \tag{38}$$

where we have used the following relations

$$P(x) = \sqrt{\frac{1}{\pi a}} \mathrm{e}^{-\frac{1}{a}x^2}, \quad H(X) = \ln \sqrt{\pi a e}, \tag{39}$$

and

$$P(x_1, x_2) = \frac{\sqrt{a^2 - b^2}}{\pi} \mathrm{e}^{-a(x_1^2+x_2^2)+2x_1x_2b}, \tag{40}$$

$$H(X_1, X_2) = \ln \frac{\mathrm{e}\pi}{\sqrt{a^2 - b^2}}, \quad a > b. \tag{41}$$

Comparing Eq. (38) with Eq. (23), it is clear that the Reid and entropic criteria lead to the same result for the TMSV state. In fact, for Gaussian states, the entropic uncertainty relation is equivalent to the Heisenberg uncertainty relation, and thus both criteria yield identical results for position–momentum measurements.[31] However, this equivalence does not generally hold for non-Gaussian states. In such cases, the entropic steering criterion typically outperforms the Reid criterion.[32,33]

3. EPR Steering under laser channel

In this section, we consider the quantum steering of continuous-variable quantum states, such as the TMSVs, when both modes propagate through a laser channel that includes both gain and loss effects. For this purpose, we start from the master equation and establish the output-input relation of the CF.

3.1. Laser channel and the output-input CF relation

For a single-mode system, the master equation describing the laser channel is given by[34]

$$\begin{aligned} \frac{\mathrm{d}}{\mathrm{d}t}\rho(t) &= g\left(2a^\dagger \rho a - aa^\dagger \rho - \rho aa^\dagger\right) \\ &\quad + \kappa\left(2a\rho a^\dagger - a^\dagger a\rho - \rho a^\dagger a\right), \end{aligned} \tag{42}$$

where g and κ are the gain and loss factors, respectively. In particular, when $g = 0$, Eq. (42) reduces to the master equation describing the amplitude decay (photon-loss) channel; for the case $g \to \kappa\bar{n}$ and $\kappa \to \kappa(\bar{n}+1)$, Eq. (42) becomes the master equation describing the thermal channel.[35]

To establish the output-input relation, we employ the entangled-state representation to obtain (see Appendix A)

$$\chi_{\mathrm{out}}(\alpha, \alpha^*) = \mathrm{e}^{-\frac{A}{2}|\alpha|^2} \chi_{\mathrm{in}}\left(\alpha \mathrm{e}^{-(\kappa-g)t}, \alpha^* \mathrm{e}^{-(\kappa-g)t}\right), \tag{43}$$

where

$$A = \Omega(1-R), \quad \Omega = \frac{\kappa+g}{\kappa-g}, \quad R = \mathrm{e}^{-2(\kappa-g)t}. \tag{44}$$

Equation (43) gives the output-input relation for any single-mode quantum state propagating through the laser channel. When both modes of a two-mode quantum state independently propagate through the laser channel, Eq. (43) leads to

$$\begin{aligned} &\chi_{\mathrm{out}}(\alpha, \alpha^*; \beta, \beta^*) = \mathrm{e}^{-\frac{A}{2}(|\alpha|^2+|\beta|^2)} \chi_{\mathrm{in}}\left(\tilde{\alpha}, \tilde{\alpha}^*; \tilde{\beta}, \tilde{\beta}^*\right), \\ &\tilde{\alpha} = \alpha \mathrm{e}^{-(\kappa-g)t}, \quad \tilde{\beta} = \beta \mathrm{e}^{-(\kappa-g)t}, \end{aligned} \tag{45}$$

where, for simplicity, symmetric laser channels are assumed, characterized by identical gain and loss factors for both modes.

3.2. TMSV under two-mode laser channel

We first consider the effects of symmetric laser channels on the steerability of the decohered TMSV (Fig. 1). Combining Eqs. (21) and (45), the output CF of the TMSV under the laser channel can be readily obtained

$$\begin{aligned} \chi_{\mathrm{out}}(q_1, p_1; q_2, p_2) &= \exp\left(-\frac{B}{2}(q_1^2 + q_2^2 + p_1^2 + p_2^2)\right) \\ &\quad \times \exp\left(C(q_1q_2 - p_1p_2)\right). \end{aligned} \tag{46}$$

where $\alpha = q_1 + \mathrm{i}p_1$, $\beta = q_2 + \mathrm{i}p_2$, and

$$B = A + R\cosh 2r, \quad C = R\sinh 2r. \tag{47}$$

Using Eqs. (5), (6), and (46), the joint position distribution and its marginal PDFs are given by

$$P(\bar{q}_1) = \frac{1}{\sqrt{\pi B}} \exp\left(-\frac{\bar{q}_1^2}{B}\right), \tag{48}$$

$$P(\bar{q}_1, \bar{q}_2) = \frac{1}{\pi\sqrt{B^2 - C^2}} \mathrm{e}^{-\frac{B\left(\bar{q}_1^2+\bar{q}_2^2\right) - 2C\bar{q}_1\bar{q}_2}{B^2-C^2}}. \tag{49}$$

The joint momentum distribution and its marginal PDFs have the same functional form as Eqs. (49) and (48), respectively, with the replacement $\bar{q}_1$, $\bar{q}_2$ by $\bar{p}_1$, $-\bar{p}_2$. From Eqs. (49) and (48), one obtains

$$H(Q_2|Q_1) = H(P_2|P_1) = \frac{1}{2}\ln\frac{\pi e(B^2-C^2)}{B}, \tag{50}$$

which leads to

$$H(Q_2|Q_1) + H(P_2|P_1) = \ln\frac{\pi e(B^2-C^2)}{B}. \tag{51}$$

On the other hand, from Eq. (46) and using Eqs. (10)–(12), the inferred variances are obtained

$$\Delta^2_{\min}(Q_2|Q_1) = \Delta^2_{\min}(P_2|P_1) = \frac{B^2-C^2}{2B}, \tag{52}$$

and consequently the steerability condition is given by

$$\Delta_{\min}(Q_2|Q_1)\,\Delta_{\min}(P_2|P_1) = \frac{B^2-C^2}{2B}. \tag{53}$$

Comparing the Reid and entropic steering conditions in Eqs. (51) and (53), one finds that they yield the same steerability condition, namely

$$B^2 - C^2 < B. \tag{54}$$

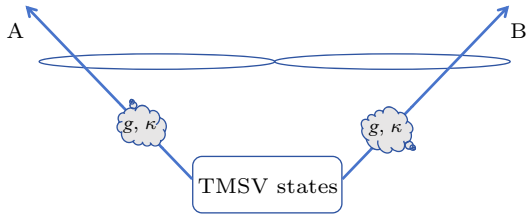


Fig. 1. The theoretical diagram of a two-mode squeezed vacuum state propagating through a laser channel.

Substituting Eqs. (44) and (47) into Eq. (54) and noticing that $A = \Omega(1-R) > 0$, we can rewrite the steerable condition as

$$aA^2 + bA - c < 0, \tag{55}$$

where we have set

$$\begin{aligned} a &= \frac{1}{\Omega^2}\left(\Omega^2 + 1 - 2\Omega\cosh 2r\right), \\ b &= \frac{1}{\Omega}\left(2\Omega\cosh 2r + \cosh 2r - 2 - \Omega\right), \\ c &= \cosh 2r - 1 = 2\sinh^2 r > 0. \end{aligned}$$

After a straightforward discussion, it is shown that the two-way steerable condition is

$$t < t_c = \frac{1}{2(\kappa - g)}\ln\left(1 + \frac{b - \sqrt{b^2+4ac}}{2\Omega a}\right)^{-1}. \tag{56}$$

Here we obtain a general expression (56) that also applies to linear amplifiers. In general, the upper bound of the evolution time t_c not only depends on the gain and loss factors, but also on the squeezing parameter. The photon-loss, photon-gain, and thermal-noise channels can be regarded as three special cases. In particular, for the photon-loss channel with $g = 0$, the steerable condition reduces to

$$\kappa t < \frac{1}{2}\ln 2. \tag{57}$$

It is interesting to note that this steerable condition is independent of the TMSV squeezing parameter, provided $r > 0$. From Eq. (57), the decohered TMSV remains steerable as long as the photon loss is less than 50%, i.e., $e^{-2\kappa t} > 1/2$. For the thermal channel, $g \to \kappa\bar{n}$ and $\kappa \to \kappa(\bar{n}+1)$. When $0 < \bar{n} < \left(e^{2r}-1\right)/2$, the steerable condition becomes

$$\kappa t < \frac{1}{2}\ln\left(\frac{2|\alpha|}{\beta + \sqrt{\beta^2 + 4|\alpha|\delta}}\right), \tag{58}$$

where $\alpha = (N+1)^2 - 4N\cosh^2 r$, $\beta = (2N-1)(\cosh 2r - N)$, $\delta = N(N-1) > 0$, and $N = (2\bar{n}+1) > 1$. In particular, when $\bar{n} = 0$, Eq. (58) reduces to Eq. (57), as expected.

Finally, we consider the case $\kappa = 0$, which yields $\Omega = -1$. From Eq. (56), we obtain

$$gt < \frac{1}{2}\ln\left(\frac{3 + \sqrt{1 + 8\tanh^2 r}}{4}\right) \leqslant \frac{1}{2}\ln\frac{3}{2}. \tag{59}$$

Equation (59) clearly shows that when gain exists in the absence of loss, the steerable condition depends on the squeezing parameter r, in contrast to the photon-loss case in Eq. (57). Interestingly, for any value of the squeezing parameter, the steerable condition is no longer satisfied once the gain exceeds a threshold, i.e., $gt > \frac{1}{2}\ln\frac{3}{2}$. This indicates that gain introduces additional noise into the TMSV, thereby destroying the steerability. In addition, comparing Eqs. (57) and (59), we find that the gain process yields a shorter steerable time when taking $g = \kappa$, with the difference between the two limits given by $\frac{1}{2}\ln\frac{4}{3}$.

3.3. One way steering

In fact, quantum steering is characterized by asymmetry, i.e., system A can steer system B, but the reverse is not necessarily true. To clearly demonstrate this asymmetry, we examine the effect of gain and loss on the steering parameters of systems A and B when the TMSV is subjected to a one-mode laser channel. Let us assume that system B (mode b) is coupled to the laser channel. In this case, according to Eq. (45), the CF of the final state is given by

$$\chi_{\text{out}}(\alpha,\alpha^*;\beta,\beta^*) = e^{-\frac{A}{2}|\beta|^2}\chi_{\text{in}}\left(\alpha,\alpha^*;\tilde{\beta},\tilde{\beta}^*\right), \tag{60}$$

and the output CF of the TMSV under the one-side laser channel is

$$\chi_{\text{TMSV}} = \exp\left(-\frac{\cosh 2r}{2}(q_1^2 + p_1^2)\right)$$

$$\times \exp\left(-\frac{B}{2}(q_2^2+p_2^2)\right)$$
$$\times \exp\left(\frac{C}{\sqrt{R}}(q_1q_2-p_1p_2)\right). \tag{61}$$

From Eq. (61) we can obtain the covariance matrix $\boldsymbol{\Sigma}$, i.e.,

$$\boldsymbol{\Sigma}=\begin{pmatrix} \cosh 2r & 0 & \frac{C}{\sqrt{R}} & 0 \\ 0 & \cosh 2r & 0 & -\frac{C}{\sqrt{R}} \\ \frac{C}{\sqrt{R}} & 0 & B & 0 \\ 0 & -\frac{C}{\sqrt{R}} & 0 & B \end{pmatrix}, \tag{62}$$

which reduces to the covariance matrix of the TMSV under ideal conditions ($t=0$), as expected. Using Eqs. (14)–(19) and (62), the steering parameters of B (mode b) and A (mode a) are given by

$$V_{B|A}=\frac{1}{4}\left(A+\frac{R}{\cosh 2r}\right)^2, \tag{63}$$
$$V_{A|B}=\frac{1}{4}\left(\frac{R+A\cosh 2r}{A+R\cosh 2r}\right)^2. \tag{64}$$

In particular, when $R=1$ ($t=0$) we have $V_{B|A}=V_{A|B}=1/(2\cosh 2r)^2$, as expected.

For the steering of B (A steering B), using Eq. (63) and noting that $R>0$ and $A>0$, the steerable condition is

$$t_{A\to B}<\frac{1}{2(\kappa-g)}\ln\left(\frac{\kappa\sinh^2 r+g\cosh^2 r}{g\cosh 2r}\right), \tag{65}$$

where the upper bound time for steering of B depends on both the loss (gain) factor and the squeezing parameter. In particular, three special cases are identified

$$\kappa t_{A\to B}<\infty,\ \text{loss}, \tag{66}$$
$$g t_{A\to B}<\frac{1}{2}\ln\left(2-\operatorname{sech}^2 r\right)<\frac{1}{2}\ln 2,\ \text{gain}, \tag{67}$$
$$\kappa t_{A\to B}<\frac{1}{2}\ln\left(\frac{N-\operatorname{sech}2r}{2\bar{n}}\right),\ \text{thermal noise}, \tag{68}$$

where $N=2\bar{n}+1$. Equations (66)–(68) correspond to the photon-loss channel ($g=0$), the photon-gain channel ($\kappa=0$), and the thermal noise channel ($g\to\kappa\bar{n}, \kappa\to\kappa(\bar{n}+1)$), respectively. It is notable that A can always steer B for arbitrarily long decoherence time if B passes only the loss channel. However, when B passes only the gain channel, there exists an upper bound $\frac{1}{2}\ln\left(2-\operatorname{sech}^2 r\right)<\frac{1}{2}\ln 2$. For the thermal noise channel, the upper bound depends on both the thermal average photon number $\bar{n}$ and the squeezing parameter r.

Similarly, for the steering of A (B steering A), we have

$$t_{B\to A}<\frac{1}{2(\kappa-g)}\ln\left(\frac{2\kappa}{\kappa+g}\right),\ (r>0), \tag{69}$$

and

$$\kappa t_{B\to A}<\frac{1}{2}\ln 2,\ \text{loss}, \tag{70}$$
$$g t_{B\to A}<\infty,\ \text{gain}, \tag{71}$$
$$\kappa t_{B\to A}<\frac{1}{2}\ln\left(\frac{2\bar{n}+2}{2\bar{n}+1}\right),\ \text{thermal noise}. \tag{72}$$

By comparing Eqs. (65) and (69), it is clear that when B passes the laser channel, the upper bound time for steering of B depends on both loss (gain) factor and squeezing parameter, whereas that for steering of A depends only on the loss (gain) factor. When B passes only the loss channel, A can steer B for any decoherence time, but B can steer A only within a threshold $\frac{1}{2}\ln 2$. Thus, the region $(0,\frac{1}{2}\ln 2)$ corresponds to two-way steering, while $(\frac{1}{2}\ln 2,\infty)$ corresponds to one-way steering.

Conversely, when B passes only the gain channel, B can steer A for any long decoherence time, while A can steer B only within the threshold $\frac{1}{2}\ln\left(2-\operatorname{sech}^2 r\right)<\frac{1}{2}\ln 2$. In this sense, the gain channel favors steering of A, whereas the loss channel favors steering of B. Accordingly, the regions $(0,\frac{1}{2}\ln\left(2-\operatorname{sech}^2 r\right))$ and $(\frac{1}{2}\ln\left(2-\operatorname{sech}^2 r\right),\infty)$ correspond to two-way and one-way steering, respectively.

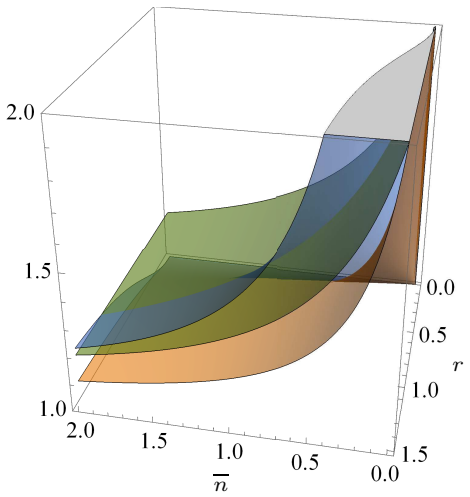


Fig. 2. Comparison of the steerable time as a function of the thermal photon number $\bar{n}$ and squeezing parameter r for one- and two-side thermal channels. The vertical axis represents $e^{2\kappa t}$. Blue (green) surfaces correspond to the one-side case, while the orange surface corresponds to the two-side case.

For the thermal channel, the upper bounds of steerable time are given by Eqs. (68) and (72) for B and A, respectively. These bounds increase with r but decrease for higher thermal noise. Notably, if the average thermal photon number $\bar{n}$ equals half of the total average photon number $\langle n\rangle=2\sinh^2 r$ of the TMSV, i.e., $\bar{n}=\langle n\rangle/2$, then A steering B and B steering A share the same upper bound. If $\bar{n}>\langle n\rangle/2$ ($\bar{n}<\langle n\rangle/2$), the latter (former) has a longer steerable time than the former (latter). This implies that one can control the direction of steering or the two-way steerable condition by tuning the ratio $\bar{n}/\langle n\rangle$, as illustrated in Fig. 2.

Next, we compare one-side and two-side decoherence. (i) For the loss case, from Eqs. (57), (66), and (70), a party without loss can steer the other with loss, while the reverse is not

true when $\kappa t > \frac{1}{2}\ln 2$, independent of r. When both parties experience photon loss, the two-way steering threshold remains unchanged, indicating that two-side loss has no greater effect on steerable time than one-side loss. (ii) For the gain case, the party with higher gain can steer the other, while the reverse is not true when $gt > \frac{1}{2}\ln\left(2-\mathrm{sech}^2 r\right)$ (dependent on r), see Eqs. (67) and (71). When both parties experience gain, one-side gain allows a longer steerable time than two-side gain, see Eqs. (59) and (67), in contrast to the loss case. (iii) For the thermal noise case, two-side channels lead to a significantly shorter steerable time than the one-side case, see Fig. 2.

4. Qualification of quantum steering in laser channel

In the discussions above, we have employed two classical steering criteria: Reid and entropy criteria. As discussed, for Gaussian states, these two criteria are equivalent and provide qualitative measures of steering. To further quantify the steerability, several measurement methods have been proposed.[36–38] In particular, for two-mode Gaussian states, characterized by the covariance matrix

$$\boldsymbol{\Sigma}_{AB} = \begin{pmatrix} \mathcal{A} & \mathcal{C} \\ \mathcal{C}^{\mathrm{T}} & \mathcal{B} \end{pmatrix}, \tag{73}$$

where $\mathcal{A}$, $\mathcal{B}$, and $\mathcal{C}$ are 2×2 submatrices, the steerability of Bob by Alice ($A\to B$) or Alice by Bob ($B\to A$) can be quantified by

$$\mathcal{G}^{A\to B} = \max\left(0,\ \frac{1}{2}\ln\frac{\det\mathcal{A}}{\det\boldsymbol{\Sigma}_{AB}}\right), \tag{74}$$

$$\mathcal{G}^{B\to A} = \max\left(0,\ \frac{1}{2}\ln\frac{\det\mathcal{B}}{\det\boldsymbol{\Sigma}_{AB}}\right). \tag{75}$$

Using Eqs. (74) and (75), we can calculate the steerability for both two-side and one-side channels, respectively, as

$$\mathcal{G}_2^{A\leftrightarrow B} = \max\left(0,\ \ln\frac{B}{B^2-C^2}\right), \tag{76}$$

and

$$\mathcal{G}_1^{A\to B} = \max\left(0,\ \ln\frac{\cosh 2r}{R+A\cosh 2r}\right), \tag{77}$$

$$\mathcal{G}_1^{B\to A} = \max\left(0,\ \ln\frac{A+R\cosh 2r}{R+A\cosh 2r}\right). \tag{78}$$

Here, the subscripts 1 and 2 denote the one-side and two-side channel cases, respectively. Comparing Eqs. (76)–(78) with Eqs. (54), (63), and (64), we observe that they share the same steerable condition, or equivalently, the same steerable time.

For the photon-gain ($\kappa = 0$) and thermal noise ($g\to\kappa\bar{n},\ \kappa\to\kappa(\bar{n}+1)$) channels, Eqs. (76)–(78) reduce to

$$\mathcal{G}_2^{A\leftrightarrow B} = \max\left(0,\ \ln\frac{R\cosh 2r - T}{(R\mathrm{e}^{2r}-T)(R\mathrm{e}^{-2r}-T)}\right), \tag{79}$$

$$\mathcal{G}_1^{A\to B} = \max\left(0,\ \ln\frac{1}{R\,\mathrm{sech}\,2r - T}\right), \tag{80}$$

$$\mathcal{G}_1^{B\to A} = \max\left(0,\ \ln\frac{R - T\,\mathrm{sech}\,2r}{R\,\mathrm{sech}\,2r - T}\right), \tag{81}$$

$$R = \mathrm{e}^{2gt},\ \ T = 1-R,$$

and

$$\mathcal{G}_2^{A\leftrightarrow B} = \max\left(0,\ \ln\frac{NT + R\cosh 2r}{(NT+R\mathrm{e}^{2r})(NT+R\mathrm{e}^{-2r})}\right), \tag{82}$$

$$\mathcal{G}_1^{A\to B} = \max\left(0,\ \ln\frac{1}{R\,\mathrm{sech}\,2r + NT}\right), \tag{83}$$

$$\mathcal{G}_1^{B\to A} = \max\left(0,\ \ln\frac{R + NT\,\mathrm{sech}\,2r}{NT + R\,\mathrm{sech}\,2r}\right), \tag{84}$$

$$R = \mathrm{e}^{-2\kappa t},\ \ T = 1-R,\ \ N = 2\bar{n}+1,$$

where when $N = 1$, Eqs. (82)–(84) reduce to the photon-loss case ($g = 0$).

To clearly illustrate the effect of different parameters on the steerability, we plot it as a function of $T = 1-R$ for the thermal channel with given parameters r and $\bar{n}$ in Fig. 3(a). From Fig. 3(a) it is evident that: (i) for a given squeezing parameter r (thermal average photon $\bar{n}$), the steerabilities $\mathcal{G}_2^{A\leftrightarrow B}$ (red), $\mathcal{G}_1^{A\to B}$ (black), and $\mathcal{G}_1^{B\to A}$ (purple) decrease (increase) with increasing $\bar{n}$ (r); (ii) for two-side and one-side photon-loss cases, although they share the same two-way steerable time (e.g., solid purple vs solid red lines), their steerabilities differ, i.e., two-side loss results in smaller steerability than one-side loss, as expected. This implies that two-side loss destroys coherence more significantly than one-side loss.

In Fig. 3(b), for the gain channel we plot steerability as a function of $1-1/R = 1-\mathrm{e}^{-2gt}$. It is observed that: (i) the more strongly gained party can steer the other party's state, while the reverse is not possible beyond a certain threshold, which depends on the squeezing parameter r. This is in sharp contrast to the less decohered party being able to steer while the other cannot. In this sense, the gain effect in one party is equivalent to the loss effect in the other party. (ii) In terms of steerable length, for a given r the relation is $\mathcal{G}_1^{B\to A} > \mathcal{G}_1^{A\to B} > \mathcal{G}_2^{A\leftrightarrow B}$, implying that two-side gain channels lead to worse steerability, since they further degrade coherence.

In general, for the laser channel, $\kappa \neq g \neq 0$, and for simplicity we define $g/\kappa = \gamma$. To clearly illustrate the effect of γ on the steerability, we plot it as a function of the dimensionless time κt for a given r and different values of γ in Fig. 4. It is found that:

(i) There exists a threshold time κt_{c} for all of $\mathcal{G}_1^{B\to A}$, $\mathcal{G}_1^{A\to B}$, and $\mathcal{G}_2^{A\leftrightarrow B}$ whenever both gain and loss are present, even in the case of $\kappa = g$.

(ii) For a given γ, the thresholds satisfy the inequality chain

$$t_{\mathrm{c}}^{A\to B} > t_{\mathrm{c}}^{B\to A} > t_{\mathrm{c}}^{A\leftrightarrow B},$$

indicating that there is always a threshold time for one-side steering ($\mathcal{G}_1^{B\to A}$ and $\mathcal{G}_1^{A\to B}$) when both gain and loss are present, in contrast to the cases with only loss or only gain. Moreover, the presence of gain and loss on both sides further shortens the threshold.

(iii) In addition, for $\mathcal{G}_1^{B\to A}$, $\mathcal{G}_1^{A\to B}$, or $\mathcal{G}_2^{A\leftrightarrow B}$, the corresponding threshold κt_c decreases with increasing γ, indicating that a larger gain g leads to a shorter threshold time.

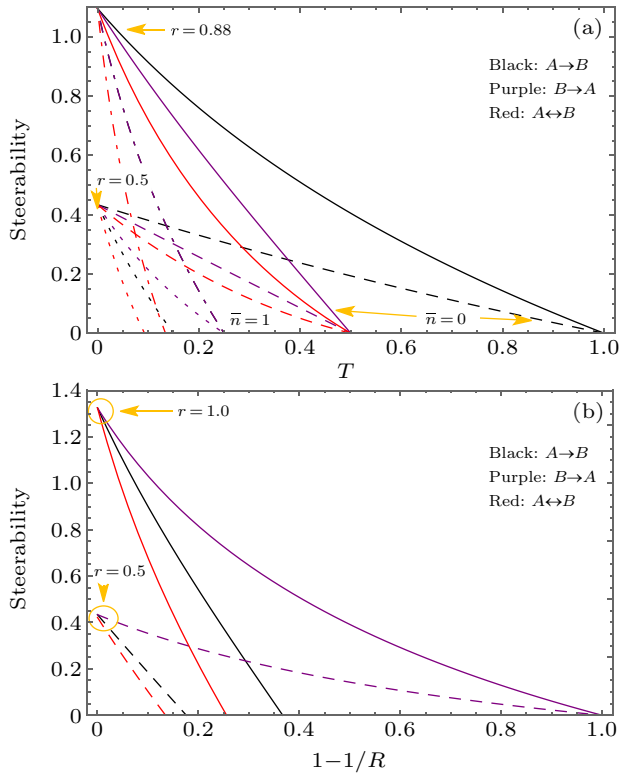


Fig. 3. Steerability as a function of $T = 1-R$ (for the thermal channel) or $1-1/R$ (for the gain channel) for selected parameters r and $\bar{n}$. (a) Thermal channel, including the photon-loss case with $R = \mathrm{e}^{-2\kappa t}$: black, purple, and red lines correspond to $\mathcal{G}_1^{A\to B}$, $\mathcal{G}_1^{B\to A}$, and $\mathcal{G}_2^{A\leftrightarrow B}$, respectively. For each color, dashed, solid, dotted, and dash-dotted lines correspond to $(r = 0.5,\ \bar{n} = 0)$, $(r = 0.88,\ \bar{n} = 0)$, $(r = 0.5,\ \bar{n} = 1)$, and $(r = 0.88,\ \bar{n} = 1)$, respectively. (b) Gain channel with $R = \mathrm{e}^{2gt}$: black, purple, and red lines correspond to $\mathcal{G}_1^{A\to B}$, $\mathcal{G}_1^{B\to A}$, and $\mathcal{G}_2^{A\leftrightarrow B}$, respectively.

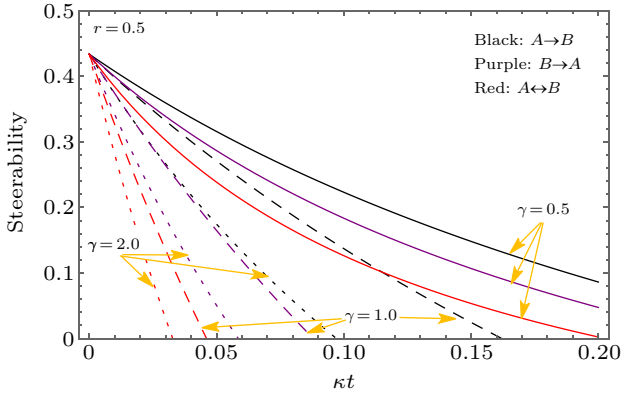


Fig. 4. Steerability as a function of κt for $r = 0.5$ and different gain-to-loss ratios $\gamma = g/\kappa = 0.5$, 1.0, and 2.0. Black, purple, and red lines correspond to $\mathcal{G}_1^{A\to B}$, $\mathcal{G}_1^{B\to A}$, and $\mathcal{G}_2^{A\leftrightarrow B}$, respectively. For each color, solid, dashed, and dotted lines correspond to $\gamma = 0.5$, 1.0, and 2.0, respectively.

5. Comparison with the decoherence of quantum entanglement

Quantum steering is a type of quantum correlation closely related to quantum entanglement and Bell nonlocality. For Gaussian states, the relationship between quantum steering and entanglement has been discussed in Ref. [4]. In this section, we further compare the decoherence of quantum steering and entanglement in a laser channel.

For two-mode Gaussian states, the degree of entanglement can be quantified by the logarithmic negativity

$$E_{\mathrm{N}} = \max(0,\ -\ln \nu_{\mathrm{s}}), \tag{85}$$

where ν_{s} is the smallest symplectic eigenvalue of the partially transposed state. The symplectic eigenvalues are defined as the modulus of the eigenvalues of the matrix $\mathrm{i}\boldsymbol{\Omega}\boldsymbol{\Sigma}$, where $\boldsymbol{\Sigma}$ is the covariance matrix (CM) of the partially transposed state, and

$$\boldsymbol{\Omega} = \begin{pmatrix} 0 & 1 \\ -1 & 0 \end{pmatrix} \oplus \begin{pmatrix} 0 & 1 \\ -1 & 0 \end{pmatrix}. \tag{86}$$

Next, we compare the decoherence of entanglement and steering under two-side and one-side channels. First, we consider the two-side case. From Eq. (46), the CM is given by

$$\boldsymbol{\Sigma}_2 = \begin{pmatrix} B & 0 & C & 0 \\ 0 & B & 0 & -C \\ C & 0 & B & 0 \\ 0 & -C & 0 & B \end{pmatrix}. \tag{87}$$

The symplectic eigenvalues are $\nu_1 = B+C$ and $\nu_2 = B-C$, so that $\nu_{\mathrm{s}} = \min(\nu_1,\ \nu_2) = B-C$. Consequently, the logarithmic negativity reads $E_{\mathrm{N}} = \max(0,\ -\ln(B-C))$, and the inseparability condition is $B-C<1$.

On the other hand, under the two-side channel condition, the steerable condition from Eq. (53) is $B-C < B/(B+C) < 1$. Comparing these two conditions, it is evident that any state satisfying the steerable condition must also satisfy the inseparability condition, while the converse is not true. This indicates that the steerable condition is stronger than the inseparability condition for characterizing quantum correlations, i.e., the steerable time is shorter than the entanglement time.

Indeed, the critical time for inseparability can be expressed as

$$t < t_{\mathrm{c}} = \frac{1}{2(\kappa-g)} \ln\left(\frac{g+\kappa\tanh r}{g(1+\tanh r)}\right), \tag{88}$$

as expected.[39] Figure 5 presents a comparison of the upper bounds on the evolution time for steering and entanglement under identical conditions. It is shown that, for the same parameters, the upper bound for entanglement is always longer than that for steering.

In particular, for the photon-loss, photon-gain, and thermal noise channels, Eq. (88) reduces to

$$\kappa t_{\mathrm{c}} \to \infty, \tag{89}$$

$$g t_{\mathrm{c}} = \frac{1}{2}\ln(1+\tanh r), \tag{90}$$

$$\kappa t_{\rm c} = \frac{1}{2}\ln\left(1+\frac{\tanh r/\bar{n}}{1+\tanh r}\right), \tag{91}$$

where Eq. (91) is also reported in Ref. [40]. As expected, these critical thresholds are longer than those corresponding to steerability.

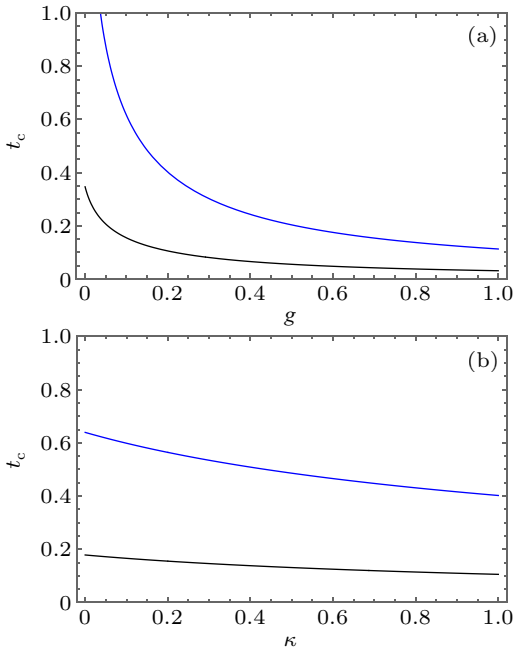


Fig. 5. Comparison of the upper bound evolution time $t_{\rm c}$ for steerability (black) and entanglement (blue) as a function of g or κ with fixed squeezing parameter $r = 0.3$. (a) Two-side channel with $\kappa = 1$; (b) Two-side channel with $g = 0.2$.

6. Single-side entanglement decoherence

We now examine the single-side case. Similarly, the degree of entanglement can be expressed as

$$E_{\rm N} = \max\left(0,\ -\ln\left(B_+ - \sqrt{B_-^2+\frac{C^2}{R}}\right)\right), \tag{92}$$

where $B_\pm = (B \pm \cosh 2r)/2$. At the initial time $t = 0$, Eq. (92) reduces to $\ln {\rm e}^{2r}$, as expected. Consequently, the inseparability condition reads

$$t < t_{\rm c} = \frac{1}{2(\kappa - g)}\ln\frac{\kappa}{g}. \tag{93}$$

Interestingly, this inseparability condition is independent of the squeezing parameter $r > 0$ when the B mode passes through the laser channel. This behavior is similar to the $A \to B$ steering case but differs from the $B \to A$ steering scenario. Moreover, the threshold $t_{\rm c}$ decreases as the gain factor g increases. In particular, for photon-loss, photon-gain, and thermal channels, Eq. (93) reduces to $\kappa t_{\rm c} \to \infty$, $g t_{\rm c} \to \infty$, and $\kappa t_{\rm c} = \frac{1}{2}\ln\frac{\bar{n}+2}{\bar{n}}$, respectively. Comparing with Eqs. (66)–(68) and (70)–(72), it is evident that the steerable condition is a subset of the inseparability condition, as expected. This can also be verified by directly comparing Eq. (93) with Eqs. (65) and (69).

7. Phase-sensitive environment

Our discussions can be extended to general noise channels. Specifically, we consider the evolution of a TMSV state under a phase-sensitive environment, which is described by the following single-mode master equation[41]

$$\begin{aligned}\frac{{\rm d}\rho}{{\rm d}t} =\ & \kappa(\bar{n}+1)\left(2a\rho a^\dagger - a^\dagger a\rho - \rho a^\dagger a\right)\\ & +\kappa\bar{n}\left(2a^\dagger\rho a - aa^\dagger\rho - \rho aa^\dagger\right)\\ & -\kappa M\left(2a^\dagger\rho a^\dagger - a^{\dagger 2}\rho - \rho a^{\dagger 2}\right)\\ & -\kappa M^*\left(2a\rho a - a^2\rho - \rho a^2\right),\end{aligned} \tag{94}$$

where M is a complex parameter characterizing the squeezed environment, satisfying $|M|^2 \le \bar{n}(\bar{n}+1)$ for a valid density operator.

Using the entangled-state representation and following the method in Eq. (43), the evolution of the CF can be written as[42] (see Appendix B)

$$\chi(\alpha,t) = \exp\left(-\frac{R}{2}\left(N|\alpha|^2 - M\alpha^{*2} - M^*\alpha^2\right)\right)\chi(\alpha\sqrt{T},0), \tag{95}$$

where $N = 2\bar{n}+1$, $R = 1-{\rm e}^{-2\kappa t}$, $T = {\rm e}^{-2\kappa t}$, and $\chi(\alpha,0)$ is the initial CF.

For an initial Gaussian state, the CF is

$$\chi(\alpha,0) = \exp\left(-\frac{1}{2}\boldsymbol{\xi}\boldsymbol{\Omega}\boldsymbol{V}_0\boldsymbol{\Omega}^{\rm T}\boldsymbol{\xi}^{\rm T}\right), \tag{96}$$

with $\boldsymbol{\xi} = (q,p)$, $\boldsymbol{V}_0$ the covariance matrix of the initial Gaussian state, and $\boldsymbol{\Omega} = \left(\begin{smallmatrix}0 & 1\\ -1 & 0\end{smallmatrix}\right)$. For simplicity, we assume zero first moments, $\bar{\xi} = 0$.

Substituting Eq. (96) into Eq. (95), the evolved covariance matrix becomes

$$\boldsymbol{V}_{\rm out} = R\boldsymbol{V}_\infty + T\boldsymbol{V}_0, \tag{97}$$

where

$$\boldsymbol{V}_\infty = \begin{pmatrix} N+2{\rm Re}M & 2{\rm Im}M\\ 2{\rm Im}M & N-2{\rm Re}M\end{pmatrix} \tag{98}$$

is the asymptotic covariance matrix as $t \to \infty$.[44–46]

Next, we consider the cases in which the TMSV passes through single-side and two-side phase-sensitive channels, respectively. Using Eq. (97), we can obtain the covariance matrix of the output state for these two cases, which takes the following form:

$$\boldsymbol{V}_j = \begin{pmatrix}\mathcal{A}_j & \mathcal{C}_j\\ \mathcal{C}_j^{\rm T} & \mathcal{B}_j\end{pmatrix}, \tag{99}$$

where the subscripts $j = 1,2$ represent single-side and two-side channels, respectively. The entanglement degree described by Eq. (99) is given by Eq. (85), with $2\nu_{\rm s}^2 = \Delta - \sqrt{\Delta^2 - 4\det\boldsymbol{V}_j}$ and $\Delta = \det\mathcal{A}_j + \det\mathcal{B}_j - 2\det\mathcal{C}_j$.

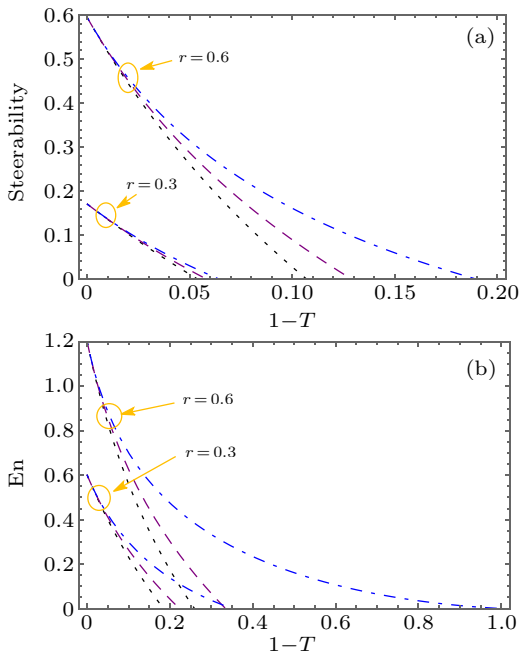


Fig. 6. Steerability and entanglement as a function of $1-T$ for given parameters $r = 0.3, 0.6$, $\bar{n} = 1$, and $M = 0, 1, \sqrt{2}$ (corresponding to black dotted, purple dashed, and blue dot-dashed lines, respectively). (a) Steerability in the two-side channel; (b) degree of entanglement.

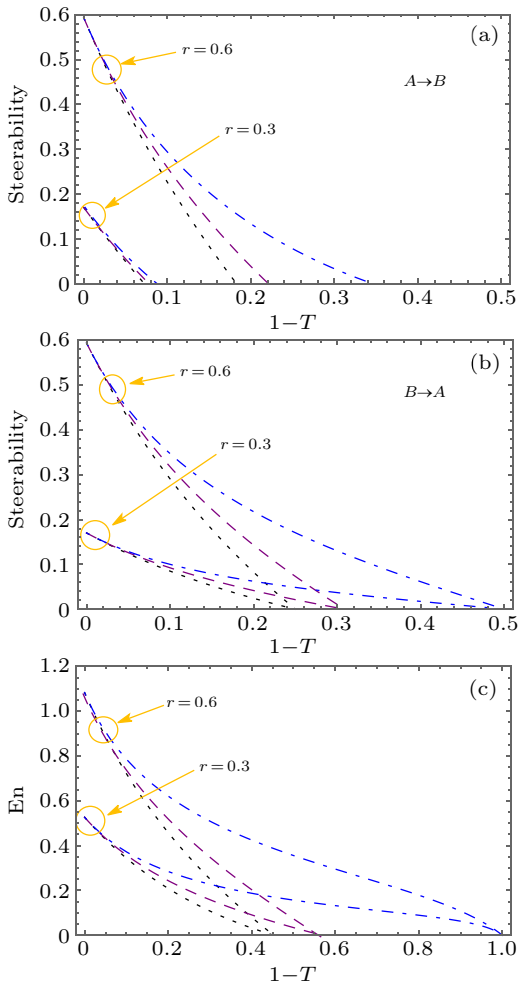


Fig. 7. Steerability and entanglement as a function of $1-T$ for given parameters $r = 0.3, 0.6$, $\bar{n} = 1$, and $M = 0, 1, \sqrt{2}$ (corresponding to black dotted, purple dashed, and blue dot-dashed lines, respectively). (a)–(b) Steerability $A \to B$ and $B \to A$; (c) degree of entanglement.

Specifically, for single- and two-side decoherence, the covariance matrices are given by

$$\boldsymbol{V}_1 = \begin{pmatrix} a_1 & 0 & d_1 & 0 \\ 0 & a_1 & 0 & -d_1 \\ d_1 & 0 & b_1+c_1 & f_1 \\ 0 & -d_1 & f_1 & b_1-c_1 \end{pmatrix}, \tag{100}$$

with $a_1 = \cosh 2r$, $b_1 = T\cosh 2r + RN$, $c_1 = 2R\mathrm{Re}\,M$, $d_1 = \sqrt{T}\sinh 2r$, $f_1 = 2R\mathrm{Im}\,M$, and

$$\boldsymbol{V}_2 = \begin{pmatrix} a_2 & c_2 & d_2 & 0 \\ c_2 & b_2 & 0 & -d_2 \\ d_2 & 0 & a_2 & c_2 \\ 0 & -d_2 & c_2 & b_2 \end{pmatrix}, \tag{101}$$

with $a_2 = R(N + 2\mathrm{Re}\,M) + T\cosh 2r$, $b_2 = R(N - 2\mathrm{Re}\,M) + T\cosh 2r$, $c_2 = 2R\mathrm{Im}\,M$, $d_2 = T\sinh 2r$.

Thus, the steerability can be calculated as

$$\mathcal{G}_1^{A\to B} = \max\left(0,\ \frac{1}{2}\ln\frac{a_1^2}{\det \boldsymbol{V}_1}\right), \tag{102}$$

$$\mathcal{G}_1^{B\to A} = \max\left(0,\ \frac{1}{2}\ln\frac{b_1^2-c_1^2-f_1^2}{\det \boldsymbol{V}_1}\right), \tag{103}$$

$$\mathcal{G}_2^{A\leftrightarrow B} = \max\left(0,\ \frac{1}{2}\ln\frac{a_2 b_2 - c_2^2}{\det \boldsymbol{V}_2}\right). \tag{104}$$

In particular, when $\bar{n} = 0$ and $M = 0$, both entanglement and steerability reduce to the previous results.

To examine the effects of phase-sensitive environments, especially the squeezing parameter M, on both entanglement and steerability, we plot them as a function of $1-T$ for several given parameters r, $\bar{n}$, and M in Figs. 6 and 7. Figures 6 and 7 correspond to two-side symmetrical decoherence channels and single-side decoherence channels, respectively.

For both cases, the presence of thermal noise further reduces both entanglement and steerability, with the reduction becoming more pronounced as $\bar{n}$ increases. For a fixed $\bar{n} = 1$, a larger squeezing parameter r enhances both entanglement and steerability initially but also leads to faster decoherence compared to smaller r.

When the squeezing environment is involved, under the condition $|M|^2 \le \bar{n}(\bar{n}+1)$, a larger M enhances entanglement and steerability more significantly. At a fixed M, the enhancement is more effective for larger r. These observations hold for both single-side and two-side decoherence cases.

Comparing Figs. 6 and 7, it is clear that entanglement and steerability perform worst under two-side decoherence. Although M enhances both quantities in both cases, the enhancement is more pronounced for the single-side case (see Figs. 7(a)–7(c)). Notably, Fig. 7(c) shows that the same decoherence time is nearly shared by different r values (0.3 and 0.6) when $M = \sqrt{2}$ ($\bar{n} = 1$), even though the smaller r yields a lower entanglement degree.

Interestingly, the decoherence time matches that without thermal noise, implying that introducing M can effectively

counteract the thermal decoherence. This is also true for A-to-B steering (see Figs. 7(a) and 7(b)). These results indicate that when only B passes through the channel: (i) the two-way steerable time can be prolonged by increasing M; (ii) even A's steering appears unaffected by thermal noise in the limit $|M|^2 = \bar{n}(\bar{n}+1)$, whereas B's steering is not fully immune.

8. Conclusion

In summary, we have studied the quantum EPR steering of two-mode continuous-variable states in a laser channel using the characteristic function representation. By varying channel parameters, we analyzed the evolution of EPR steering in loss, gain, and thermal channels. Concretely, we showed that the bound of two-way steerable time depends not only on the gain and loss factors but also on the squeezing parameter in the laser channel, whereas the squeezing parameter does not influence the bound in the pure loss channel.

Furthermore, we found that the gain process introduces additional noise to the two-mode squeezed vacuum states, thereby reducing the steerable time under both single-mode and two-mode laser channels. When only the B system passes through a gain channel, B can always steer A for arbitrarily long decoherence times, while A can steer B only within a threshold time–opposite to the behavior observed in loss channels. By comparing steerable and inseparable conditions, we showed that the steerable condition can be regarded as a subset of the inseparable condition.

Finally, we extended our analysis to phase-sensitive environments. Our results establish benchmarks for implementing tasks such as quantum entanglement distribution over noisy channels and provide insights into mitigating noise to enable reliable quantum communication protocols. For instance, these findings suggest promising directions for designing quantum steering distillation schemes to enhance the robustness of quantum information processing under realistic conditions. Overall, this work deepens our understanding of quantum communication in imperfect environments and opens new avenues for practical quantum technology development.

Appendix A: Derivation of Eq. (43)

Here we derive Eq. (43) using the thermal entangled state representation method. For this purpose, we introduce a state vector

$$|I\rangle = \exp\left\{a^\dagger \tilde{a}^\dagger\right\}|0\tilde{0}\rangle = \sum_{m=0}^{\infty}|m,\tilde{m}\rangle, \tag{A1}$$

where $m=\tilde{m}$, and $a^\dagger$ and $\tilde{a}^\dagger$ are the creation operators of the real and fictitious modes, satisfying $[\tilde{a},\tilde{a}^\dagger]=1$ and $\tilde{a}|0\tilde{0}\rangle = 0$. The thermal entangled state representation is obtained by displacing the real mode

$$\begin{aligned}|\eta\rangle &= D_a(\eta)|0\tilde{0}\rangle \\ &= \exp\left(-\frac{|\eta|^2}{2}+\eta a^\dagger - \eta^*\tilde{a}^\dagger + a^\dagger\tilde{a}^\dagger\right)|0\tilde{0}\rangle, \end{aligned}\tag{A2}$$

where $D_a(\eta)=\exp\{\eta a^\dagger - \eta^* a\}$ is the displacement operator for mode a. The state $|\eta\rangle$ satisfies the eigen-equations

$$(a-\tilde{a}^\dagger)|\eta\rangle = \eta|\eta\rangle, \quad (a^\dagger - \tilde{a})|\eta\rangle = \eta^*|\eta\rangle, \tag{A3}$$

and similarly for the bra

$$\langle\eta|(a^\dagger-\tilde{a}) = \eta^*\langle\eta|, \quad \langle\eta|(a-\tilde{a}^\dagger) = \eta\langle\eta|. \tag{A4}$$

When $\eta=0$, we have

$$a|I\rangle = \tilde{a}^\dagger|I\rangle, \quad \tilde{a}|I\rangle = a^\dagger|I\rangle, \quad a^\dagger a|I\rangle = \tilde{a}^\dagger\tilde{a}|I\rangle. \tag{A5}$$

Next, we relate the CF and $\langle\eta|$. By definition, $\chi(\lambda) = \mathrm{tr}[\mathrm{e}^{\lambda a^\dagger - \lambda^* a}\rho]$, which can be rewritten as

$$\begin{aligned}\chi(\lambda) &= \sum_{m,n=0}^{\infty}\langle n,\tilde{n}|\mathrm{e}^{\lambda a^\dagger-\lambda^* a}\rho|m,\tilde{m}\rangle \\ &= \langle I|D_a(\lambda)|\rho\rangle \\ &= \langle\eta=-\lambda|\rho\rangle, \end{aligned}\tag{A6}$$

where $|\rho\rangle \equiv \rho|I\rangle$.

To derive Eq. (43), we operate Eq. (42) on $|I\rangle$ and use Eq. (A5), giving

$$\begin{aligned}\frac{\mathrm{d}}{\mathrm{d}t}|\rho(t)\rangle &= \Big[g(2a^\dagger\tilde{a}^\dagger - aa^\dagger - \tilde{a}\tilde{a}^\dagger) \\ &\quad +\kappa(2a\tilde{a}-a^\dagger a-\tilde{a}^\dagger\tilde{a})\Big]|\rho(t)\rangle \\ &= \Big[(\kappa+g)(\tilde{a}-a^\dagger)(a-\tilde{a}^\dagger) \\ &\quad +(\kappa-g)(a\tilde{a}-a^\dagger\tilde{a}^\dagger+1)\Big]|\rho(t)\rangle. \end{aligned}\tag{A7}$$

Acting on $\langle\eta=-\lambda|$ and using

$$\langle\eta|\tilde{a} = -\Big(\frac{\partial}{\partial\eta}+\frac{\eta^*}{2}\Big)\langle\eta|, \tag{A8}$$

$$\langle\eta|\tilde{a}^\dagger = \Big(\frac{\partial}{\partial\eta^*}-\frac{\eta}{2}\Big)\langle\eta|, \tag{A9}$$

$$\langle\eta|a = \Big(\frac{\partial}{\partial\eta^*}+\frac{\eta}{2}\Big)\langle\eta|, \tag{A10}$$

$$\langle\eta|a^\dagger = -\Big(\frac{\partial}{\partial\eta}-\frac{\eta^*}{2}\Big)\langle\eta|, \tag{A11}$$

we obtain

$$\begin{aligned}\frac{d}{dt}\chi(\lambda) &= -(\kappa-g)\Big(\eta\frac{\partial}{\partial\eta}+\eta^*\frac{\partial}{\partial\eta^*}\Big)\chi(\lambda) \\ &\quad -(\kappa+g)|\eta|^2\chi(\lambda). \end{aligned}\tag{A12}$$

Its solution is

$$\begin{aligned}\chi(\lambda,t) &= \exp\left[-(\kappa+g)t|\eta|^2-(\kappa-g)t\Big(\eta\frac{\partial}{\partial\eta}+\eta^*\frac{\partial}{\partial\eta^*}\Big)\right] \\ &\quad\times\chi(\lambda,0), \end{aligned}\tag{A13}$$

with $\eta = -\lambda$. Using the operator identity

$$e^{f(A+\sigma B)} = e^{\sigma B(e^{f\tau}-1)/\tau} e^{fA}, \quad [A,B] = \tau B, \tag{A14}$$

and noting $[\eta\partial_\eta + \eta^*\partial_{\eta^*}, \eta^*\eta] = 2\eta\eta^*$, Eq. (A13) reduces to

$$\begin{aligned}\chi(\lambda,t) \;=\; & \exp\Big[-\frac{1}{2}\frac{\kappa+g}{\kappa-g}\big(1-e^{-2(\kappa-g)t}\big)|\eta|^2\Big] \\ & \times\chi(\lambda e^{-(\kappa-g)t},0),\end{aligned} \tag{A15}$$

which is Eq. (43), as expected.

Appendix B: Derivation of Eq. (95)

In a manner similar to the derivation of Eq. (43), we first rewrite Eq. (94) as

$$\begin{aligned}\frac{d|\rho\rangle}{dt} \;=\; & \kappa\Big\{(\bar{n}+1)\Big[(a-\tilde{a}^\dagger)\tilde{a}+(\tilde{a}-a^\dagger)a\Big] \\ & +\bar{n}\Big[(a^\dagger-\tilde{a})\tilde{a}^\dagger+(\tilde{a}^\dagger-a)a^\dagger\Big] \\ & -M(a^\dagger-\tilde{a})^2-M^*(\tilde{a}^\dagger-a)^2\Big\}|\rho\rangle,\end{aligned} \tag{B1}$$

and then, using Eqs. (A8)–(A11), the CF equation becomes

$$\frac{d}{dt}\chi(\lambda,t) = -\kappa\Big(G+\eta\frac{\partial}{\partial\eta}+\eta^*\frac{\partial}{\partial\eta^*}\Big)\chi(\lambda,t), \tag{B2}$$

where

$$G = (2\bar{n}+1)|\eta|^2 - M\eta^{*2} - M^*\eta^2. \tag{B3}$$

Using the operator identity in Eqs. (A14) and (A15), we then obtain the solution

$$\chi(\lambda,t) = \exp\Big(-\frac{1}{2}(1-e^{-2\kappa t})G\Big)\chi(\lambda e^{-\kappa t},0), \tag{B4}$$

as expected.

Acknowledgments

This work was supported by the National Natural Science Foundation of China (Grant Nos. 12404410, 12564049, 11964013, and 61975077), the National Key Research and Development Program of China (Grant No. 2024ZD0300900), and the Jiangxi Provincial Natural Science Foundation (Grant No. 20242BAB26009).

References

[1] Schrödinger E 1935 *Math. Proc. Cambridge Philos. Soc.* **31** 555
[2] Reid M, Drummond P, Bowen W, Cavalcanti E G, Lam P K, Bachor H, Andersen U L and Leuchs G 2009 *Rev. Mod. Phys.* **81** 1727
[3] Gallego R and Aolita L 2015 *Phys. Rev. X* **5** 041008
[4] He Q, Gong Q and Reid M 2015 *Phys. Rev. Lett.* **114** 060402
[5] Cavalcanti D and Skrzypczyk P 2016 *Rep. Prog. Phys.* **80** 024001
[6] Uola R, Costa A C, Nguyen H C and Gühne O 2020 *Rev. Mod. Phys.* **92** 015001
[7] Wiseman H M, Jones S J and Doherty A C 2007 *Phys. Rev. Lett.* **98** 140402
[8] Meng H X, Zhou J, Jiang S H, Xu Z P, Ren C, Su H Y and Chen J L 2018 *Opt. Commun.* **425** 101
[9] Armstrong S, Wang M, Teh R Y, Gong Q, He Q, Janousek J, Bachor H A, Reid M D and Lam P K 2015 *Nat. Phys.* **11** 167
[10] Sun K, Ye X J, Xu J S, Xu X Y, Tang J S, Wu Y C, Chen J L, Li C F and Guo G C 2016 *Phys. Rev. Lett.* **116** 160404
[11] Deng X, Xiang Y, Tian C, Adesso G, He Q, Gong Q, Su X, Xie C and Peng K 2017 *Phys. Rev. Lett.* **118** 230501
[12] Tischler N, Ghafari F, Baker T J, *et al.* 2018 *Phys. Rev. Lett.* **121** 100401
[13] Cavaillès A, Le Jeannic H, Raskop J, Guccione G, Markham D, Diamanti E, Shaw M D, Verma V B, Nam S W and Laurat J 2018 *Phys. Rev. Lett.* **121** 170403
[14] Weston M M, Slussarenko S, Chrzanowski H M, Wollmann S, Shalm L K, Verma V B, Allman M S, Nam S W and Pryde G J 2018 *Sci. Adv.* **4** e1701230
[15] Saunders D J, Jones S J, Wiseman H M and Pryde G J 2010 *Nat. Phys.* **6** 845
[16] Sun K, Xu J S, Ye X J, Wu Y C, Chen J L, Li C F and Guo G C 2014 *Phys. Rev. Lett.* **113** 140402
[17] Li C M, Chen K, Chen Y N, Zhang Q, Chen Y A and Pan J W 2015 *Phys. Rev. Lett.* **115** 010402
[18] Handchen V, Eberle T, Steinlechner S, Samblowski A, Franz T, Werner R F and Schnabel R 2012 *Nat. Photonics* **6** 596
[19] Qin Z, Deng X, Tian C, Wang M, Su X, Xie C and Peng K 2017 *Phys. Rev. A* **95** 052114
[20] Wang N, Wang M, Tian C, Deng X and Su X 2023 *Laser Photon. Rev.* **18** 2300653
[21] Rosales-Zárate L, Teh R, Kiesewetter S, Brolis A, Ng K and Reid M 2015 *J. Opt. Soc. Am. B* **32** A82
[22] Deng X, Liu Y, Wang M, Su X and Peng K 2021 *npj Quantum Inf.* **7** 65
[23] Wang F, Wang C, Shen K and Hu X 2022 *Opt. Express* **30** 15830
[24] Liu Y, Zheng K, Kang H, Han D, Wang M, Zhang L, Su X and Peng K 2022 *npj Quantum Inf.* **8** 38
[25] Wang Y, Hao Z Y, Li J K, Liu Z H, Sun K, Xu J S, Li C F and Guo G C 2023 *Phys. Rev. Lett.* **130** 200202
[26] Zhang Q X, Fang X X and Lu H 2024 *Photon. Res.* **12** 552
[27] González-Raya T, Pirandola S and Sanz M 2024 *Commun. Phys.* **7** 126
[28] Mehrabankar S, Mahmoudi P, Abbasnezhad F, Afshar D and Isar A 2024 *Quantum Inf. Process.* **23** 343
[29] Białynicki-Birula I and Mycielski J 1975 *Commun. Math. Phys.* **44** 129
[30] Walborn S, Salles A, Gomes R, Toscano F and Ribeiro P S 2011 *Phys. Rev. Lett.* **106** 130402
[31] Wolf M M, Giedke G and Cirac J I 2006 *Phys. Rev. Lett.* **96** 080502
[32] Lee C W, Ji S W and Nha H 2013 *J. Opt. Soc. Am. B* **30** 2483
[33] Chowdhury P, Pramanik T, Majumdar A S and Agarwal G S 2014 *Phys. Rev. A* **89** 012104
[34] Da C and Fan H Y 2019 *Chin. J. Phys.* **62** 1
[35] Gardiner C W and Zoller P 2000 *Quantum Noise* (New York: Springer)
[36] Skrzypczyk P, Navascués M and Cavalcanti D 2014 *Phys. Rev. Lett.* **112** 180404
[37] Kogias I, Lee A R, Ragy S and Adesso G 2015 *Phys. Rev. Lett.* **114** 060403
[38] Jevtic S, Hall M J, Anderson M R, Zwierz M and Wiseman H M 2015 *J. Opt. Soc. Am. B* **32** A40
[39] Poon P S Y and Law C K 2007 *Phys. Rev. A* **76** 012333
[40] Duan L M, Giedke G, Cirac J I and Zoller P 2000 *Phys. Rev. Lett.* **84** 2722
[41] Serafini A, Illuminati F, Paris M G A and De Siena S 2004 *Phys. Rev. A* **69** 022318
[42] Chen F and Fan H 2012 *Sci. China Phys. Mech. Astron.* **55** 2076
[43] Weedbrook C, Pirandola S, García-Patrón R, Cerf N J, Ralph T C, Shapiro J H and Lloyd S 2012 *Rev. Mod. Phys.* **84** 621
[44] Lütkenhaus N, Cirac J I and Zoller P 1998 *Phys. Rev. A* **57** 548
[45] Paris M G A, Illuminati F, Serafini A and De Siena S 2003 *Phys. Rev. A* **68** 012314
[46] Kim M S and Imoto N 1995 *Phys. Rev. A* **52** 2401